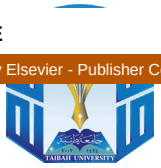

Journal of Taibah University for Science 10 (2016) 345–351

www.elsevier.com/locate/jtusci

Liquefied petroleum gas sensing by Al-doped TiO_2 nanoparticles synthesized by chemical and solid-state diffusion routes

K.R. Nemade [a,c,*], R.V. Barde [b,c], S.A. Waghuley [b,c]

[a] *Department of Applied Physics, J D College of Engineering and Management, Nagpur 441 501, India*
[b] *Department of Engineering Physics, H.V.P.M. College of Engineering and Technology, Amravati 444605, India*
[c] *Department of Physics, Sant Gadge Baba Amravati University, Amravati 444 602, India*

Available online 4 April 2015

Abstract

In the current study, we synthesized an Al-doped TiO_2 nanoceramic material using a chemical and solid-state diffusion routes, and the LPG sensing performance of this material was comparatively studied. The structural conformation of the as-synthesized nanoparticles was investigated using X-ray diffraction (XRD) analysis, and the morphology was analysed by scanning electron microscopy (SEM). The optical absorption spectrum of the as-synthesized nanoparticles was recorded by ultraviolet–visible spectroscopy. Thermal study of the samples was performed via thermogravimetric analysis (TGA). Based on a comparison of both samples, the chemically synthesized Al-doped TiO_2 nanoparticle exhibited good sensor performance for LPG. The material synthesized by the chemical route exhibited good sensing properties.

Keywords: Liquefied petroleum gas; Al-doped TiO_2; Solid-state diffusion

1. Introduction

LPG has a wide variety of applications in various fields, such as domestic, agriculture and industry. In addition, LPG can be utilized as a cooking fuel. Because LPG is composed of hydrocarbons, it causes indoor air pollution resulting in detrimental affects on human health (i.e., irritated respiratory tract, nose and eyes). Therefore, its detection becomes necessary at lower concentrations to avoid accidents.

Verma et al. [1] studied the LPG sensing characteristics of iron titanium oxide thin films, which was also employed as an opto-electronic humidity sensor. Parveen et al. [2] synthesized a polyaniline–titanium dioxide nanocomposite for LPG sensing. Yadav et al. [3] reported a solid-state titania for use as a LPG gas sensor at room temperature. Singh et al. reported the LPG sensing characteristics of $Zn_xCu_{1-x}Fe_2O_4$ ($0.0 \leq x \leq 0.8$) nanocomposites. In this study, the effect of the zinc concentration on the magnetic properties was also investigated using a vibrating sample magnetometer. The results of this study indicated that the samples are more selective and sensitive towards LPG than CO_2 gas [4]. Singh et al. demonstrated the room

* Corresponding author at: Department of Applied Physics, J D College of Engineering and Management, Nagpur 441 501, India. Tel.: +91 9049703051; fax: +91 0712548975.
E-mail address: krnemade@gmail.com (K.R. Nemade).
Peer review under responsibility of Taibah University.

Production and hosting by Elsevier

http://dx.doi.org/10.1016/j.jtusci.2015.03.003

temperature sensing application of zinc ferrite nanorods for LPG. In this investigation, more variations in the electrical resistance were observed for LPG than for CO_2 gas, which indicates that the samples are more selective and sensitive towards LPG [5]. Jaiswal et al. studied the enhancement of the gas sorption ability of a LPG sensor. This study concluded that mesoporosity plays a crucial role in enhancing the sorption capability of thin films [6]. Tsai et al. [7] prepared Al-doped TiO_2 ceramic nanoparticles by a single-step direct combination of vaporized Ti, Al and O_2, and these nanoparticles exhibited visible-light photocatalytic activity. Tsai et al. [8] also prepared a high-quality Al-doped TiO_2 visible-light photocatalyst by combination of vaporized Ti, Al and O_2 using a 6 kW thermal plasma system. Liu et al. [9] demonstrated the synthesis of an aluminium-doped TiO_2 mesoporous material using a solid-state reaction with cetyltrimethylammonium bromide as a template agent and tetrabutyl orthotitanate as a precursor. Kumar et al. [10] studied the reflectivity and photostability of Al-doped TiO_2 nanoparticles synthesized by a sol–gel method. Li et al. [11] demonstrated p-type hydrogen sensing with an Al-doped TiO_2 nanostructure.

In the current study, we synthesized Al-doped TiO_2 nanoparticles by two different routes (i.e., chemical and solid-state diffusion) and studied their LPG sensing characteristics. To the best of our knowledge, no studies on the LPG sensing ability of Al-doped TiO_2 nanoparticles have been reported. In addition, we investigated the LPG sensing response characteristics at concentration levels up to 400 ppm. The operating temperature was determined to be 448 K, which is much lower than the auto-ignition temperature of LPG.

2. Experimental

2.1. Chemical route

AR grade chemicals were used in this study without further purification. Aluminium nitrate ($Al(NO_3)_3{\cdot}9H_2O$) and titanium dioxide (TiO_2) were used as starting chemicals. First, 0.2 M $Al(NO_3)_3{\cdot}9H_2O$ was added to 1 M TiO_2 under constant magnetic stirring using an organic media (i.e., methanol). This mixture was maintained at room temperature overnight for complete removal of the methanol. The as-obtained product was sintered at 600 °C.

2.2. Solid state diffusion route

The Al-doped TiO_2 nanoparticles were prepared by a solid-state diffusion route using the starting chemicals (i.e., $Al(NO_3)_3{\cdot}9H_2O$ and TiO_2). 0.2 M $Al(NO_3)_3{\cdot}9H_2O$ was mixed directly with 1 M TiO_2 using an agate mortar and pestle. The crushed sample was pre-sintered at 400 °C for 2 h and crushed again in a mortar and pestle. The as-obtained product was sintered at 800 °C for 6 h. Finally, the sample in the crucible was allowed to cool to room temperature.

2.3. Characterization of materials and gas sensing measurements

The structural purity of the as-synthesized nanomaterials was analysed by X-ray diffraction (XRD) analysis carried out on a Rigaku miniflex-II X-ray diffractometer in a 2θ range of 10–70°.

The topography of the samples was observed using scanning electron microscopy (SEM) on a JEOL JSM-7500F. The optical absorption curve for the Al-doped TiO_2 nanoparticles was acquired using an Agilent 8453 UV-Visible-NIR Spectrophotometer. The thermal study of the samples was performed using thermogravimetric analysis (TGA) with a Shimadzu DTG-60 h thermal analyser under a nitrogen atmosphere.

The sensing films of the as-prepared samples were prepared by a screen-printing technique on SiO_2 substrate with a size of 25 mm × 25 mm using a binding agent (composed of butyl carbitol and ethyl cellulose) [12]. The ohmic contacts were deposited on the sensing film. The gas sensing responses of the as-synthesized materials were analysed by a specially designed sensing unit. The sensing characteristics were studied using air as a background gas. The selected volume of the LPG was inserted into the chamber to maintain the required concentration inside the chamber. The voltage drop method was utilized to measure the resistance change as a function of the LPG concentration [13]. The sensing response of the films is defined as [14]:

$$S = \frac{\Delta R}{R_a} = \frac{|R_g - R_a|}{R_a} \quad (1)$$

where R_a and R_g are the resistances of chemiresistor in air and gas, respectively.

3. Results and discussion

3.1. Structural analysis and surface morphological studies

Fig. 1 shows the XRD pattern of TiO_2 and the Al-doped TiO_2 nanoparticles synthesized by the chemical and solid-state diffusion routes. The position of the diffraction peaks in the pattern and the relative intensity

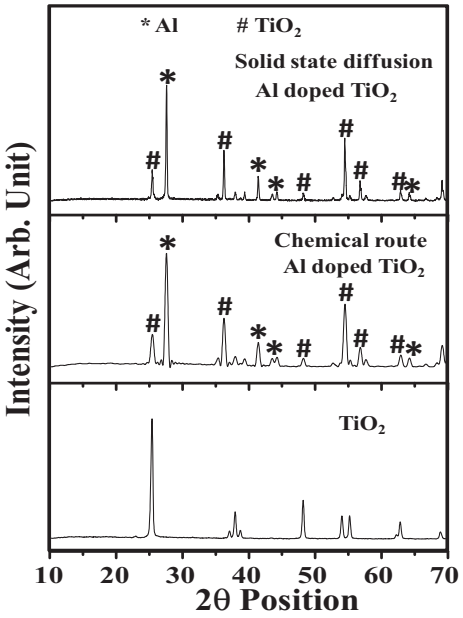

Fig. 1. XRD pattern of the Al-doped TiO_2 nanoparticles synthesized by chemical and solid-state diffusion routes.

data are in agreement with ICDD File card no. 01-084-1285 for anatase TiO_2. The characteristics peaks of the Al-doped TiO_2 system are indicated in a symbolic manner. The XRD patterns of the Al-doped TiO_2 nanoparticles synthesized by the chemical and solid-state diffusion routes are also in excellent agreement with the parent TiO_2 with the characteristics peaks of aluminium. Some characteristics peaks of aluminium were suppressed, which indicates that Al is nicely doped in the TiO_2 structure. These peaks corresponding to aluminium were indexed to ICDD card no. 01-081-1667. More broadening of the diffraction peaks was observed for the Al-doped TiO_2 nanoparticles synthesized by the chemical route. According to Scherrer's equation, the size of the Al-doped TiO_2 nanoparticles prepared by the chemical route are smaller than the particles synthesized by the solid-state diffusion route [15]. This increase in the particle size in the solid-state diffusion route is due to the annealing temperature because the increase in temperature may result in merging of the particles [16].

Because the Al-doped TiO_2 belongs to the tetragonal system, the lattice constants are computed using Eq. (2).

$$\frac{1}{d^2} = \frac{h^2 + k^2}{a^2} + \frac{l^2}{c^2} \tag{2}$$

where a and c are the lattice constants and d is the lattice spacing. In comparison to anatase TiO_2, the doping of Al into TiO_2 results in an increased in the a lattice parameter and a decrease in the c lattice parameter. This

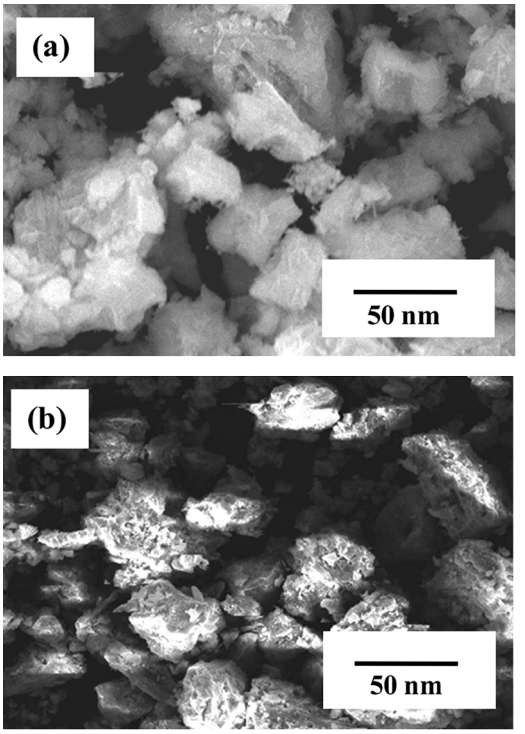

Fig. 2. SEM images of the Al-doped TiO_2 nanoparticles synthesized by (a) chemical and (b) solid-state diffusion routes.

change in the lattice parameters results in a decrease in the particle size with increasing Al concentration [17]. The lattice parameters estimated for the Al-doped TiO_2 system synthesized by both routes are summarized in Table 1.

Based on the results in Table 1, the a lattice parameter is larger than that for the chemically synthesized Al-doped TiO_2 nanoparticles. Using Scherrer's equation, the average crystallite sizes were determined to be 21.6 and 24.8 nm for the material prepared by the chemical and solid-state diffusion routes, respectively. This decrease in the size for the particles prepared by the chemical route may be due to a lower annealing temperature and an increase in the lattice parameters. The smaller particle size provides a larger area for the adsorption of gas molecules, which results in improved sensing.

Fig. 2(a) and (b) shows the SEM images of the Al-doped TiO_2 nanoparticles synthesized by the chemical

Table 1
Lattice parameters of the Al-doped TiO_2 nanoparticles.

Synthesis route	a (Å)	b (Å)	c (Å)
Chemical route	4.5943	4.5943	2.9584
Solid state diffusion route	4.5929	4.5929	2.9604

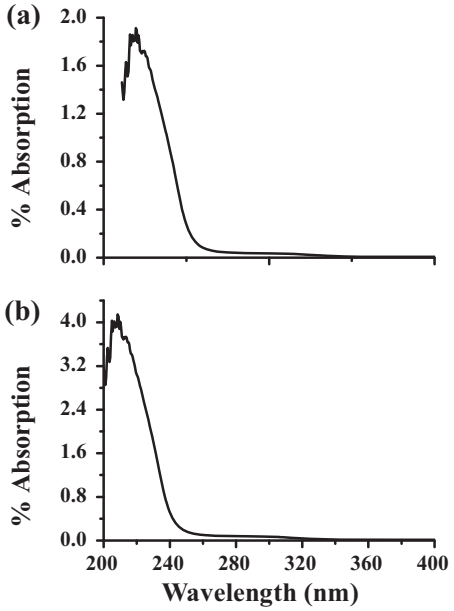

Fig. 3. UV–Vis spectrum of the Al-doped TiO_2 nanoparticles synthesized by (a) chemical and (b) solid-state diffusion routes.

and solid-state diffusion routes, respectively. The particles synthesized by the chemical route have a flat surface and exhibit a small amount of aggregation. However, the particles synthesized by the solid-state diffusion route have fluffy surfaces with a rough morphology. The rough morphology is not preferable for gas sensing applications. The particle size calculated using XRD analysis is in good agreement with that obtained in the SEM study.

3.2. Optical and thermal study of Al-doped TiO_2 nanoparticles

Fig. 3(a) and (b) shows the UV–Vis spectrum of the Al-doped TiO_2 nanoparticles synthesized by the chemical and solid-state diffusion routes. The as-synthesized samples exhibit an intense absorption in the UV region at approximately 230–240 nm, which indicates that this material exhibits quantum confinement [18].

Fig. 4 shows the direct band gap plot for the Al-doped TiO_2 nanoparticles. The direct band gap of the Al-doped TiO_2 nanoparticles synthesized by the chemical route is larger than that for the nanoparticles prepared by the solid-state diffusion route. According to the hyperbolic band model and effective mass approximation model, the band gap and particle size are inversely related to each other [19]. Therefore, the band gap of the Al-doped TiO_2 nanoparticles is larger when prepared by the chemical route, which produces a smaller average particle

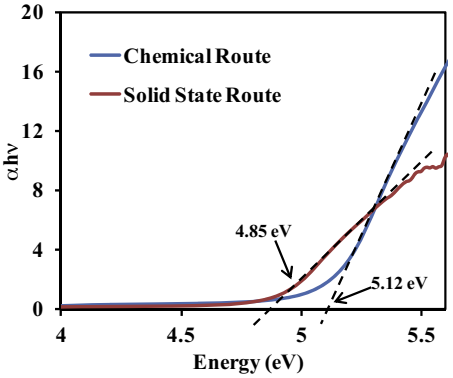

Fig. 4. Plot of the energy as a function of ($\alpha h\nu$) of the Al-doped TiO_2 nanoparticles.

size. This conclusion based on the UV–Vis results is consistent with the previous XRD and SEM analyses.

Fig. 5 shows the TGA plot for the Al-doped TiO_2 nanoparticles synthesized by the chemical and solid-state diffusion routes. The results indicate that significant weight loss was observed up to 450 K. At temperatures higher than 450 K, no weight loss was observed, and the curve plateaus to 800 K. Thermal analysis indicates that the sample acquires thermal stability from 440 to 800 K. Similarly, the operating temperature of the sensors lies in this range, which is favourable for LPG detection.

3.3. LPG sensing response

Fig. 6 shows the selectivity response of Al-doped TiO_2 towards CO_2 and LPG at a concentration of

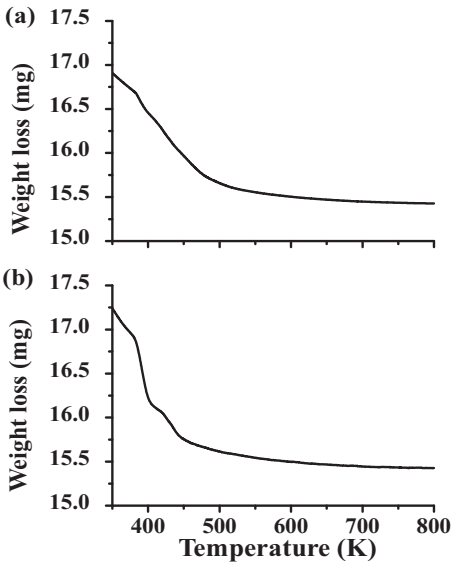

Fig. 5. TGA curve for the Al-doped TiO_2 nanoparticles synthesized by (a) chemical and (b) solid-state diffusion routes.

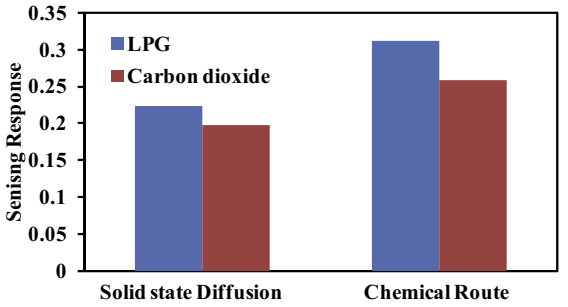

Fig. 6. Selectivity response of Al-doped TiO_2 towards CO_2 and LPG.

400 ppm and room temperature. Both samples are more selective towards LPG. Therefore, additional investigation of gas sensing is only focused on the LPG response.

Fig. 7 shows the LPG sensing response of the Al-doped TiO_2 nanoparticles at room temperature. Based on the plot, the Al-doped TiO_2 nanoparticles synthesized by the chemical route exhibit a higher sensing response. When the Al-doped TiO_2 nanoparticles are exposed LPG, the sensor resistance decreases. The sensing response curve is nearly linear at lower concentrations of LPG but deviates from linearity at higher concentrations. In the current study, Al was doped into TiO_2 as a sensitizer, which result in the formation of highly reactive species. This type of reactive species is useful in efficient gas sensing. The interaction between Al and adsorbed oxygen species can be expressed as

$$O_2 + Al_3 \rightarrow 3Al : O \quad (3)$$

In this surface reaction, the Al atoms weakly interact with atmospheric oxygen. Therefore, the resulting species that form on the surface readily dissociate even at room temperature. In this case, oxygen captures electrons from LPG, which are added to the sensing surface.

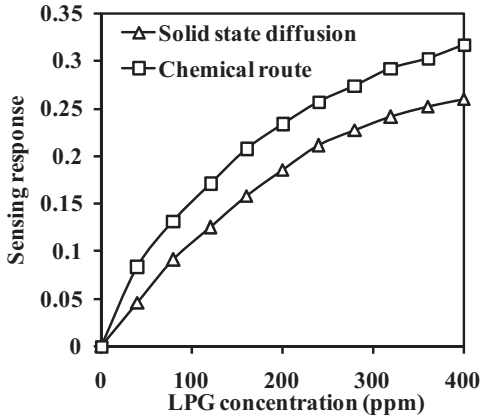

Fig. 7. LPG sensing response of the as-synthesized Al-doped TiO_2 nanoparticles.

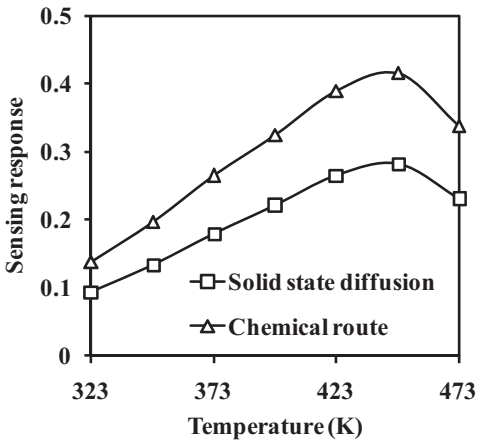

Fig. 8. Operating temperature response of the Al-doped TiO_2 nanoparticles.

This addition of electrons into the conduction band of the sensing surface results in a decrease in the resistance [20]. The interaction between LPG and Al-doped TiO_2 via adsorbed oxygen can be expressed as

$$C_nH_{2n+2} + 2O^-(ads) \rightarrow H_2O + C_nH_{2n}: O + e^- \quad (4)$$

$$C_nH_{2n}: O + O^-(ads) \rightarrow CO_2 + H_2O + e^- \quad (5)$$

In this surface reaction, electrons are generated due to the formation of H_2O and CO_2.

Fig. 8 shows the operating temperature response for Al-doped TiO_2 towards a fixed concentration (200 ppm) of LPG. The response curve indicates an optimum value at 448 K, which may be due to the large adsorption rate of atmospheric oxygen on the sensing surface resulting in enhancement of the sensing response. Beyond a certain temperature, the response value starts to decrease, which is due to the desorption of adsorbed oxygen molecules from the sensing surface. At a higher temperature, oxygen detaches from the surface due to an increase in thermal vibrations.

Fig. 9 shows the transient response of the Al-doped TiO_2 nanoparticles for 200 ppm LPG at room temperature. The rapid response (32 s) and recovery time (40 s) were determined from the plot for both samples. The recovery time is greater than the response time, which may be due to the formation of H_2O and CO_2 on the sensing surface. These species require longer periods of time to dissociate. Therefore, the recovery time is greater than the response time. Fig. 10 shows the stability response for 15 days, which is nearly linear indicating the good stability of the sample to LPG. This good stability may be due to the stable structure of the nanoparticles [21]. Based on these sensing parameters, these sensing films can be effectively used as LPG sensors.

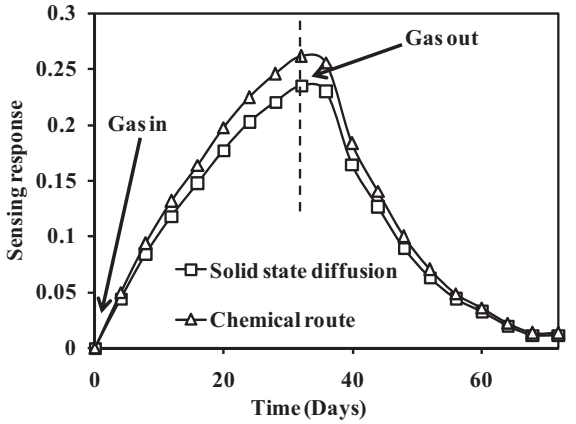

Fig. 9. Transient response characteristics of the Al-doped TiO_2 nanoparticles towards LPG.

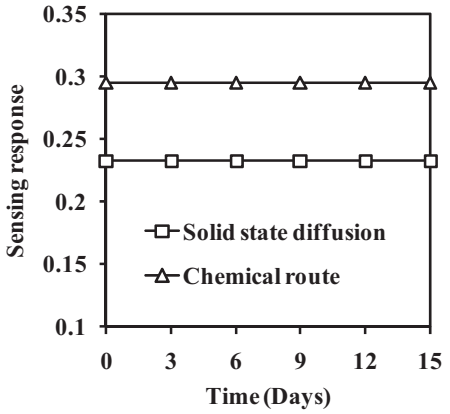

Fig. 10. Stability response of the Al-doped TiO_2 nanoparticles against LPG.

4. Conclusions

In summary, we successfully synthesized Al-doped TiO_2 nanoparticles using two different routes (i.e., chemical and solid-state diffusion routes). The XRD pattern confirmed the formation and structural purity of the as-synthesized materials. SEM and UV–Vis analyses indicated that the particle size was smaller for the material obtained by the chemical route. This analysis is in good agreement with the XRD study. The Al-doped TiO_2 nanoparticles synthesized by the chemical route exhibit high selectivity, sensitivity and stability towards LPG. The operating temperature of the fabricated sensor was determined to be 448 K, which is much lower than the autoignition temperature of LPG. The good performance of the Al-doped TiO_2 nanoparticles synthesized by the chemical route was due to the smaller particle size.

Acknowledgements

The authors wish to thank the Head of the Department of Physics, Sant Gadge Baba Amravati University, Amravati for providing the necessary facilities. One of the authors, Kailash Nemade, wishes to thank Prof. P.B. Maheshwari, Prof. S.M. Bang and Prof. N.H. Patil, Directors, J D College of Engineering and Management, Nagpur.

References

[1] N. Verma, S. Singh, R. Srivastava, B.C. Yadav, Fabrication of iron titanium oxide thin film and its application as opto-electronic humidity and liquefied petroleum gas sensors, Opt. Laser Technol. 57 (2014) 181–188.
[2] A. Parveen, A. Koppalkar, A.S. Roy, Liquefied petroleum gas sensing of polyaniline–titanium dioxide nanocomposites, Sens. Lett. 11 (2012) 242–248.
[3] B.C. Yadav, A. Yadav, T. Shukla, S. Singh, Solid-state titania-based gas sensor for liquefied petroleum gas detection at room temperature, Bull. Mater. Sci. 34 (2011) 1639–1644.
[4] A. Singh, S. Singh, B.D. Joshi, A. Shukla, B.C. Yadav, P. Tandon, Synthesis, characterization, magnetic properties and gas sensing applications of $Zn_xCu_{1-x}Fe_2O_4$ ($0.0 \leq x \leq 0.8$) nanocomposites, Mater. Sci. Semicond. Process. 27 (2014) 934–949.
[5] A. Singh, A. Singh, S. Singh, P. Tandon, B.C. Yadav, R.R. Yadav, Synthesis, characterization and performance of zinc ferrite nanorods for room temperature sensing applications, J. Alloys Compd. 618 (2015) 475–483.
[6] A.K. Jaiswal, S. Singh, A. Singh, R.R. Yadav, P. Tandon, B.C. Yadav, Fabrication of Cu/Pd bimetallic nanostructures with high gas sorption ability towards development of LPG sensor, Mater. Chem. Phys. 154 (2015) 16–21.
[7] C. Tsai, H. Hsi, H. Bai, K.S. Fan, H. Sun, Single-step synthesis of Al-doped TiO_2 nanoparticles using non-transferred thermal plasma torch, Jpn. J. Appl. Phys. 51 (2012), 01AL01–01AL06.
[8] C. Tsai, T. Kuo, H. His, Fabrication of Al-doped TiO_2 visible-light photocatalyst for low-concentration mercury removal, Int. J. Photoenergy 2012 (2012) 874509–874517.
[9] S. Liu, G. Liu, Q. Feng, Al-doped TiO_2 mesoporous materials: synthesis and photodegradation properties, J. Porous Mater. 17 (2010) 197–206.
[10] S. Kumar, N.K. Verma, M.L. Singla, Study on reflectivity and photostability of Al-doped titania nanoparticles and their reflectors, J. Mater. Res. 28 (2013) 521–528.
[11] Z. Li, D. Ding, C. Ning, Ni-doped TiO_2 nanotubes for wide-range hydrogen sensing, Nanoscale Res. Lett. 9 (2013) 118–127.
[12] K.R. Nemade, S.A. Waghuley, Chemiresistive gas sensing by few-layered graphene, J. Electron. Mater. 42 (2013) 2857–2866.
[13] K.R. Nemade, S.A. Waghuley, Low operable temperature chemiresistive gas sensing by graphene–zinc oxide quantum dots composites, Sci. Adv. Mater. 6 (2014) 128–134.
[14] K.R. Nemade, S.A. Waghuley, LPG sensing application of graphene/Bi_2O_3 quantum dots composites, Solid State Sci. 22 (2013) 27–32.
[15] K.R. Nemade, S.A. Waghuley, LPG sensing application of graphene/CeO_2 quantum dots composite, AIP Conf. Proc. 1536 (2013) 1258–1259.

[16] A. Gaber, M.A. Abdel-Rahim, A.Y. Abdel-Latief, M.N. Abdel-Salam, Influence of calcination temperature on the structure and porosity of nanocrystalline SnO_2 synthesized by a conventional precipitation method, Int. J. Electrochem. Sci. 9 (2014) 81–95.

[17] L. Xu, M.P. Garrett, B. Hu, Doping effects on internally coupled seebeck coefficient, electrical, and thermal conductivities in aluminum-doped TiO_2, J. Phys. Chem. C 116 (2012) 13020–13025.

[18] K.R. Nemade, S.A. Waghuley, UV–VIS spectroscopic study of one pot synthesized strontium oxide quantum dots, Results Phys. 3 (2013) 52–54.

[19] K.R. Nemade, S.A. Waghuley, Low temperature synthesis of semiconducting α-Al_2O_3 quantum dots, Ceram. Int. 40 (2014) 6109–6113.

[20] V.R. Shinde, T.P. Gujar, C.D. Lokhande, Enhanced response of porous ZnO nanobeads towards LPG: effect of Pd sensitization, Sens. Actuators B 123 (2007) 701–706.

[21] K.V. Gurav, P.R. Deshmukh, C.D. Lokhande, LPG sensing properties of Pd-sensitized vertically aligned ZnO nanorods, Sens. Actuators B 151 (2011) 365–369.